

## The impact of climate change and anthropogenic activities on alpine grassland over the Qinghai-Tibet Plateau



Baoxiong Chen<sup>a,b</sup>, Xianzhou Zhang<sup>a,\*</sup>, Jian Tao<sup>a</sup>, Jianshuang Wu<sup>a</sup>,  
Jingsheng Wang<sup>a</sup>, Peili Shi<sup>a</sup>, Yangjian Zhang<sup>a</sup>, Chengqun Yu<sup>a</sup>

<sup>a</sup> Lhasa Plateau Ecosystem Research Station, Key Laboratory of Ecosystem Network Observation and Modeling, Institute of Geographic Sciences and Natural Resources Research, Chinese Academy of Sciences, Beijing 100101, China

<sup>b</sup> Graduate University of Chinese Academy of Sciences, Beijing 100049, China

### ARTICLE INFO

#### Article history:

Received 28 August 2013  
Received in revised form  
28 December 2013  
Accepted 3 January 2014

#### Keywords:

The Qinghai-Tibet plateau  
Alpine grassland ecosystem  
Net primary production  
Climate change  
Anthropogenic activities

### ABSTRACT

Climate change and anthropogenic activities are two factors that have important effects on the carbon cycle of terrestrial ecosystems, but it is almost impossible to fully separate them at present. This study used process-based terrestrial ecosystem model to stimulate the potential climate-driven alpine grassland net primary production (NPP), and Carnegie–Ames–Stanford Approach based on remote sensing to stimulate actual alpine grassland NPP influenced by both of climate change and anthropogenic activities over the Qinghai–Tibet plateau (QTP) from 1982 to 2011. After the models were systematically calibrated, the simulations were validated with continuous 3-year paired field sample data, which were separately collected in fenced and open grasslands. We then simulated the human-induced NPP, calculated as the difference between potential and actual NPP, to determine the effect of anthropogenic activities on the alpine grassland ecosystem. The simulation results showed that the climate change and anthropogenic activities mainly drove the actual grassland NPP increasing in the first 20-year and the last 10-year respectively, the area percentage of actual grassland NPP change caused by climate change from 79.62% in the period of 1982–2001 to 56.59% over the last 10 years; but the percentage change resulting from human activities doubled from 20.16% to 42.98% in the same periods over the QTP. The effect of human activities on the alpine grassland ecosystem obviously intensified in the latter period compared with the former 20 years, so the negative effect caused by climate change to ecosystem could have been relatively mitigated or offset over the QTP in the last ten years.

© 2014 Elsevier B.V. All rights reserved.

### 1. Introduction

Both global climate change and anthropogenic activities are the main driving forces of terrestrial ecosystems (Esser, 1987; Field, 2001; Haberl, 1997). Commonly, regional ecosystem changes are the consequence of both climate change and local anthropogenic activities, but it is almost impossible to directly differentiate between these two factors (Wessels et al., 2007). Especially in arid and semi-arid areas, heightened anthropogenic activities can easily lead to the degradation of certain ecosystems, even causing serious ecological and economical losses (Harris, 2010; Wessels et al., 2004). With the increase in climate warming and intensified anthropogenic activities over the last century (Consortium, 2013; Raupach et al., 2013), socioeconomic drivers are beginning to overwhelm the great forces of nature for some selected processes regionally or even on the global scale (Erb et al., 2009; Luck, 2007;

Rojstaczer et al., 2001). As a result, separating and quantifying the influence of climate change and human activities on ecosystems has great significance to ecosystem management and adaptation; Thus, mankind can choose different adaptive management strategies to adapt to climate change or to counteract the negative effect of anthropogenic activities on ecosystems (Aldous et al., 2011; Lawler, 2009; Vignola et al., 2009). Therefore, it is imperative to use an objective and reproducible method to discriminate between the effects of climate change and anthropogenic activities on ecosystems (Wessels et al., 2008).

At present, the ways for indirectly evaluating the regional influence of anthropogenic activities on ecosystems include the Normalized Difference Vegetation Index (NDVI) residual trend method (Bai et al., 2008; Li et al., 2012; Wessels et al., 2004), and human appropriation of net primary productivity (HANPP) method based on models (DeFries, 2002; Haberl et al., 2007; Rojstaczer et al., 2001; Xu et al., 2009). Some studies reported that the NDVI significantly correlated with rainfall in arid and semi-arid areas, so the deviation between the actual and simulated NDVI can be regarded as the human activities effect on the ecosystem (Prince et al., 2007;

\* Corresponding author. Tel.: +86 10 6488 9690; fax: +86 10 6485 4230.

E-mail address: [zhangxz@igsnrr.ac.cn](mailto:zhangxz@igsnrr.ac.cn) (X. Zhang).

[Wessels et al., 2004, 2007, 2008](#)). Study on the temperate grassland in Inner Mongolia in China showed that the governmental ecological protection strategy applied after 2000 in this area significantly resulted in large-scale vegetation improvements ([Li et al., 2012](#)), but there are existing uncertainties about the rain-production relationship, and the climatic and anthropogenic influences on the ecosystem still cannot be fully differentiated. Otherwise, the alternative methods for simulating HANPP applied social statistical models ([Krausmann et al., 2013; Rojstaczer et al., 2001; Vitousek et al., 1986](#)) or required much social statistical data to simulate the human and actual productivity, which can easily lead to results uncertainties ([DeFries, 2002; DeFries et al., 1999; Haberl et al., 2007; Xu et al., 2009](#)). Another possible method is that comparing the process-based and remote-sensing ecosystem productivity models to simulate the human-induced production, which can be then used for trend analysis and avoiding uncertainties in some extent.

As the sole and largest geographical unit with the highest elevation on earth, the Qinghai-Tibet plateau (QTP) is called the “Third Pole” and acts as an important reservoir for water, regulating climate change and water resources in east Asia and even for the whole world ([Qiu, 2008; Yang et al., 2011; Yao et al., 2012](#)). The QTP also has a large variety of ecosystem types, from subtropical rain forest in southeast to alpine desert in the northwest. Among all types of land cover vegetation, alpine grassland is the dominant ecosystem over the QTP, covering more than 50% of the whole plateau area ([Bartholomé and Belward, 2005; Gao et al., 2012](#)). With both global climate warming and increasing anthropogenic activities, the QTP has experienced approximately a three times increase of the global warming rate over the last 50 years ([Piao et al., 2011; Qiu, 2008](#)). Meanwhile, natural grassland has been regionally degrading since the 1980s, which may be due to a combination of climate warming, increasing population, fast-growing grazing pressure and rodent damage ([Harris, 2010; Liu et al., 2012; Wang et al., 2013; Yu et al., 2012](#)). Regardless of the exact reason of ecosystem degrading, the local government is facing a serious issue in managing the vast grasslands in view of such complicated environmental problems ([Du et al., 2004; Qiu, 2007; Yu et al., 2012](#)). Although, recent studies have shown that the QTP has changed from a small or neutral carbon source to a carbon sink during the 20th century, and net primary production (NPP) simulation has been persistently enhanced over the last 50 years ([Piao et al., 2012; Zhuang et al., 2010](#)), but it is still hard to determine where and how serious anthropogenic activities influences grassland NPP in such a large scale. Nonetheless, alpine grassland is sensitive to climate warming and anthropogenic activities, so the QTP is the ideal place for studying the relationship between climate warming and the anthropogenic activities effects on alpine grassland.

In this study, our objective was to distinguish between the effects of climate change and anthropogenic activities on alpine grassland over the QTP, and trying to determine which is the main driving force for grassland ecosystem change over different time periods. We used grassland NPP as the index for measuring the degree of climate change and anthropogenic activities effects on the alpine grassland ecosystem, with a climate factor-driven model to simulate grassland potential NPP and a remote sensing model to simulate the actual NPP, which is affected by both of climate change and human activities, so the human-induced NPP is modelled as the difference of potential and actual NPP. For comparing the trend of the potential and human-induced NPP over periods, the main driving force to ecosystem change can be determined. This study could be used as a reproducible method for quantifying the impact of climate change and anthropogenic activities on terrestrial ecosystem NPP change and provide a theoretical basis for optimizing ecosystem management over rangelands.

## 2. Methods and data

### 2.1. Methods

The Terrestrial Ecosystem Model (TEM) was used to simulate the climatic potential NPP ( $NPP_P$ ), which is the maximum grassland NPP and only driven by climatic factors and unaffected by human activities. The Carnegie-Ames-Stanford Approach (CASA) model was used to simulate actual NPP ( $NPP_A$ ), which is the actual existing NPP that was influenced by both climate change and human activities, for the remote-sensing NDVI data represent the actual vegetation greenness. So, the human-induced NPP ( $NPP_H$ ) only affected by human activities can be simulated in corresponding to timescales as follows:

$$NPP_H = NPP_P - NPP_A \quad (1)$$

The TEM is a widely used process-based ecosystem model that simulates the carbon and nitrogen dynamics of plants and soils within terrestrial ecosystems ([Melillo et al., 1993; Raich et al., 1991; Tian et al., 1998; Zhuang et al., 2010](#)). It is driven by spatially referenced information on vegetation type, climate, elevation, soils, and water availability to calculate the monthly carbon and nitrogen fluxes and pool sizes of terrestrial ecosystems. The formula for calculating monthly NPP is as follows:

$$GPP = (C_{max}) \frac{PAR}{PAR + k_i} \frac{C_i}{k_c + C_i} (TEMP)(KLEAF) \quad (2)$$

$$NPP_P = GPP - R_a = GPP - (R_m + R_g) \quad (3)$$

where  $C_{max}$  is the maximum rate of carbon assimilation under optimal environmental conditions, which is determined according to vegetation types; PAR is the photosynthetically active radiation at canopy level;  $k_i$  is the irradiance at which carbon assimilation proceeds at one-half its maximum rate;  $C_i$  is the concentration of  $CO_2$  inside leaves;  $k_c$  is the internal  $CO_2$  concentration at which assimilation proceeds at one-half its maximum rate; TEMP and KLEAF are unitless multipliers expressing the influences of air temperature and plant phenology. The GPP is the ecosystem gross primary production, assuming that the conversion efficiency of photosynthate to biomass is 100%, and the  $NPP_P$  is estimated as the GPP minus the  $R_a$  (autotrophic respiration), which includes  $R_m$  (maintenance respiration) and  $R_g$  (growth respiration) ([Raich et al., 1991](#)). In this study, we mainly calibrated TEM parameters of  $C_{max}$  as  $949.6 \text{ g C m}^{-2} \text{ month}^{-1}$  for alpine meadow,  $617.9 \text{ g C m}^{-2} \text{ month}^{-1}$  for alpine steppe and  $251.2 \text{ g C m}^{-2} \text{ month}^{-1}$  for alpine desert steppe, and the ratio of photosynthetically active radiation (PAR) to solar global radiation as 0.44 ([Raich et al., 1991; Zhang et al., 2000; Zhou et al., 2004](#)).

The CASA model was developed to estimate NPP on a large geographical scale, based on remote sensing and climatic data ([Field et al., 1995; Gao et al., 2013; Potter, 1999, 2004; Potter et al., 1993, 1999, 2011](#)). In the model, the simulation was determined by two variables: absorbed photosynthetically active radiation (APAR) and light energy conversion ( $\varepsilon$ ), as follows:

$$NPP_A = APAR \times \varepsilon = fPAR \times PAR \times \varepsilon^* \times T_\varepsilon \times W_\varepsilon \quad (4)$$

where fPAR is the fraction of the incoming PAR intercepted by green vegetation, which is calculated from the NDVI image dataset;  $\varepsilon^*$  is the maximum possible light energy conversion efficiency, this term was set uniformly at  $0.55 \text{ g CMJ}^{-1} \text{ PAR}$  ([Potter et al., 2011](#)); and  $T_\varepsilon$  and  $W_\varepsilon$  are unitless varying scalar terms for temperature ( $T$ ) and water ( $W$ ).

Formula (5) was used to calculate the long-term grassland NPP changing trend;  $n$  represents the sequential years and the  $NPP_i$  is the NPP in the year  $i$ . A positive slope value suggests that the NPP is in an increasing trend while a negative one indicates that the

**Table 1**

The causes of actual NPP<sub>A</sub> change and its corresponding to mathematical methods. Note: the sNPP<sub>A</sub>, sNPP<sub>P</sub> and sNPP<sub>H</sub> represent the absolute slope value for NPP<sub>A</sub>, NPP<sub>P</sub> and NPP<sub>H</sub> change trend in every pixel.

Method (comparing slope)	Cause of NPP change
sNPP <sub>A</sub> = 0	NPP <sub>A</sub> has no change (NC)
sNPP <sub>A</sub> > 0 and sNPP <sub>P</sub> > sNPP <sub>H</sub>	NPP <sub>A</sub> increase due to climate change (ICC)
sNPP <sub>A</sub> > 0 and sNPP <sub>P</sub> < sNPP <sub>H</sub>	NPP <sub>A</sub> increase due to human activities (IHA)
sNPP <sub>A</sub> < 0 and sNPP <sub>P</sub> > sNPP <sub>H</sub>	NPP <sub>A</sub> decrease due to climate change (DCC)
sNPP <sub>A</sub> < 0 and sNPP <sub>P</sub> < sNPP <sub>H</sub>	NPP <sub>A</sub> decrease due to human activities (DHA)

NPP is decreasing; then a slope of zero means that the NPP shows no change trend and remains steady (Ma et al., 2006; Stow et al., 2003). In this study, the relative slope ( $\bar{s}_i$ ) in Formula (6) was used to indicate the relative NPP change in every pixel point.

$$\text{Slope} = \frac{n \times \sum_{i=1}^n (i \times \text{NPP}_i) - \sum_{i=1}^n i \times \sum_{i=1}^n \text{NPP}_i}{n \times \sum_{i=1}^n i^2 - (\sum_{i=1}^n i)^2} \quad (5)$$

$$\bar{s}_i = \frac{\text{slope}_i}{(1/n) \times \sum_{i=1}^n \text{NPP}_i} \quad (6)$$

In order to determine the reasons of NPP<sub>A</sub> change in every pixel, the absolute slope values of the NPP<sub>P</sub> and NPP<sub>H</sub> in the same period were compared for defining the causes of NPP<sub>A</sub> change. Table 1 shows the five types of different conditions that leading to NPP<sub>A</sub> change.

## 2.2. Data

In this study, an advanced very high resolution radiometer (AVHRR) NDVI dataset developed by the Global Inventory Modeling and Mapping Studies (GIMMS) group (<http://glcf.umd.edu/data/gimms/>) was processed for simulating the NPP<sub>A</sub>. This dataset has a spatial resolution of 8 km and a temporal resolution of 15 days intervals, available online from 1982 to 2006. Also, the moderate-resolution imaging spectroradiometer (MODIS) NDVI product (MYD13A2.5) with a spatial resolution of 1 km and a temporal scale of 16 days can be obtained from the website [https://lpdaac.usgs.gov/get\\_data/data\\_pool](https://lpdaac.usgs.gov/get_data/data_pool), which covers images from 2001 to 2011. All the remote-sensing data for the QTP were downloaded and composited as a monthly data set using the maximum value composite (MVC) method. For reducing the residual noise caused by haze and clouds, the 432 composited NDVI images were cleaned by employing an adaptive Savitzky–Golay smoothing filter, using the TIMESAT package (Jiang et al., 2012; Jönsson and Eklundh, 2004).

The meteorological data were collected from the China Meteorological Administration (<http://www.cma.gov.cn/>) via permanent meteorological stations across China. 200 long-term observing stations with complete monthly meteorological records from 1982 to 2011 for the QTP and its around were selected, and interpolated the meteorological data by using ANUSPLIN version 4.2 software to form monthly raster data layers with spatial resolutions of 1 km and 8 km.

During the course of the investigation in the north of the QTP, we sampled both fenced and open alpine grassland paired in different places with various grassland types—in the summer from 2009 to 2011 continuously. The collected dataset included 108 sites (5 plots per site) of alpine grassland above- and below-ground biomass; further details of the sampling methods can be found in other publications (Li et al., 2011; Wu et al., 2013). Then we calculated the NPP from the collected grass biomass data, assuming that the above-ground biomass as the accumulated above-ground NPP, which is about equal to the below-ground NPP and about half of the total NPP (Wu et al., 2009).

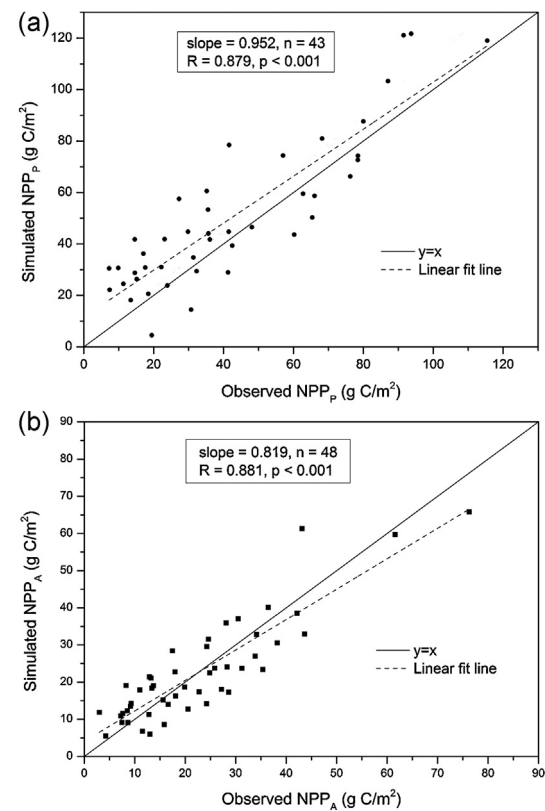


Fig. 1. Comparisons of TEM-simulated NPP<sub>P</sub> and CASA-simulated NPP<sub>A</sub> with the observed NPP data in the year of 2009, 2010, and 2011; (a) NPP<sub>P</sub> and observed fenced grassland data and (b) NPP<sub>A</sub> and observed open grassland data.

## 3. Results

### 3.1. Validation of NPP

We used the fenced grassland sample NPP data to calibrate the parameters of the TEM and validate the simulations, meanwhile the open grassland sample data was used to validate the CASA simulation. Comparisons of the results showed that the simulated NPP data matched well with the observed data from 2009 to 2011 ( $P < 0.001$ ) and can be used in the following analysis. Fig. 1 showed that the regression linear slope of the NPP<sub>P</sub> against sampled fenced

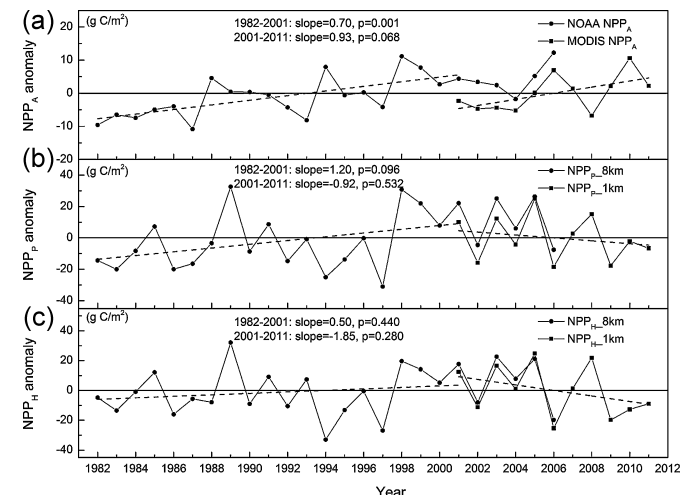
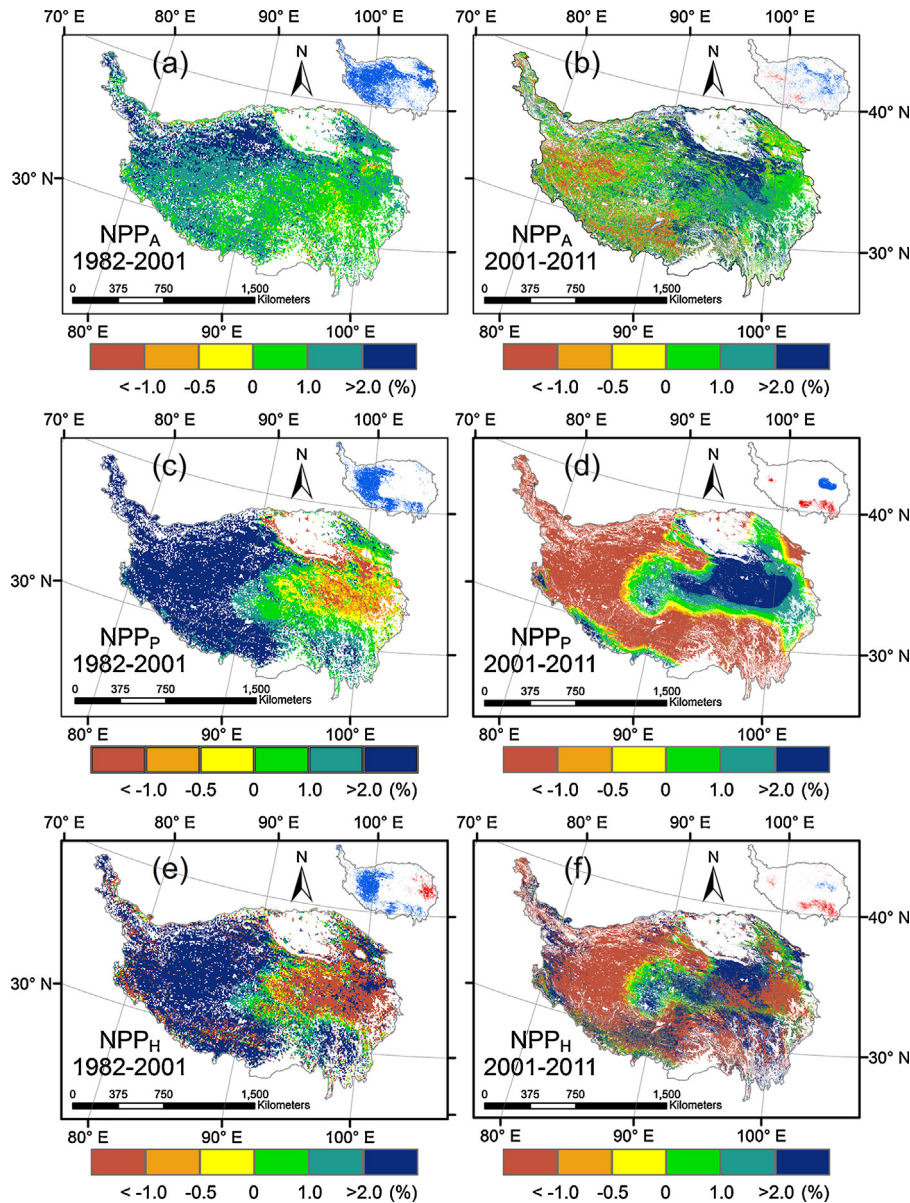


Fig. 2. Inter-annual variation in anomalies of: (a) CASA-modeled NPP<sub>A</sub>, (b) TEM-modeled NPP<sub>P</sub>, and (c) NPP<sub>H</sub> over the QTP alpine grasslands from 1982 to 2011.



**Fig. 3.** Spatial distributions of (a–f) trends in annual NPP over the QTP grasslands in the periods 1982–2001 and 2001–2011. (a) NPP<sub>A</sub> simulation from 1982 to 2001, (b) NPP<sub>A</sub> simulation from 2001 to 2011, (c) NPP<sub>P</sub> simulation from 1982 to 2001, (d) NPP<sub>P</sub> simulation from 2001 to 2011, (e) NPP<sub>H</sub> simulation from 1982 to 2001, (f) NPP<sub>H</sub> simulation from 2001 to 2011. The inset maps show significant ( $P < 0.05$ ) NPP increase (blue), and significant ( $P < 0.05$ ) NPP decrease (red). (For interpretation of the references to color in this figure legend, the reader is referred to the web version of this article.)

grassland NPP is 0.952, with 43 points, and the coefficient reaches 0.879 (Fig. 1a); Fig. 1b showed that the regression slope of the NPP<sub>A</sub> against observed open grassland NPP is 0.819, with 48 sample points, and the coefficient is 0.881 (Fig. 1b).

### 3.2. NPP<sub>A</sub> change over the QTP

The simulated results showed that the alpine grassland NPP<sub>A</sub> over the QTP increased in the past thirty years, but shared different increasing rate in the two periods of 1982–2001 and 2001–2011 (Fig. 2 a). From 1982 to 2001, the simulated NPP<sub>A</sub> increased with a rate of about  $0.70 \text{ g C m}^{-2} \text{ yr}^{-1}$  (Fig. 2a), with a significantly total increase of 16.83% ( $P < 0.01$ ). The NPP<sub>A</sub> increment mainly occurred in the north and west of the QTP, as well as a small area in the middle-east, but the north margin appeared to be following a decreasing trend (Fig. 3 a). In the period 2001–2011, the

NPP<sub>A</sub> increased with a rate of  $0.93 \text{ g C m}^{-2} \text{ yr}^{-1}$  (Fig. 2a), with a NPP<sub>A</sub> increase of 8.05%. In this period, the NPP<sub>A</sub> decrement mostly occurred in the west and southwest of the QTP, while the increment occurred in the east (Fig. 3b).

Because of that the NPP<sub>A</sub> in the two periods were simulated using different remote-sensing NDVI data sources with varied spatial resolutions, so there existed a systematic difference between the two periodic simulations. In the overlapped time from 2001 to 2006, the simulation results showed a disproportionate deviation between the two remote sensing data driven NPP<sub>A</sub> (Fig. 2a), which is possibly caused by the 2001–2006 GIMMS NDVI datasets quality over western QTP (Zhang et al., 2013a). So, the overlapped time simulations for NPP<sub>A</sub> based on GIMMS NDVI dataset and its corresponding NPP<sub>P</sub> and NPP<sub>H</sub> simulations from 2001 to 2006 are not analyzed in this study for avoiding the uncertainties.

### 3.3. $NPP_p$ and $NPP_h$ change over the QTP

The  $NPP_A$  change relates to the  $NPP_p$  and  $NPP_h$ , and its change trend is determined by the change trend of  $NPP_p$  and  $NPP_h$  according to the formula 1. For the alpine grassland over the QTP, both of the  $NPP_p$  and  $NPP_h$  showed increasing trends in 1982–2001 as the model simulations, but with decreasing trends in 2001–2011 with different slopes (Fig. 2). Fig. 2b and c illustrated the annual variation in anomalies of  $NPP_p$  and  $NPP_h$  from 1982 to 2001, when the  $NPP_p$  increased by  $1.20 \text{ g Cm}^{-2} \text{ yr}^{-1}$  (Fig. 2b) and mainly occurred in the south and west of the QTP, but it showed a declined trend in the middle and eastern areas (Fig. 3c). The  $NPP_h$  was also enhanced at a rate of  $0.50 \text{ g Cm}^{-2} \text{ yr}^{-1}$  in this period (Fig. 2c), and most of the increments occurred in the middle west and north of the QTP, with decreasing in the south and middle east (Fig. 3e). In this twenty years period, the increasing rate of  $NPP_p$  change is greater than that of  $NPP_h$  variation, which suggested that effect of climate change on alpine grassland ecosystem over the QTP is larger than that of human activities, and the increased  $NPP_h$  cannot offset the enhanced climate change influence, so  $NPP_A$  increased from 1982 to 2001.

However, the mechanism has changed in the latter period from 2001 to 2011. On account of the continuous drought caused by climate warming over the QTP,  $NPP_p$  was in a decreasing trend with the rate of  $-0.92 \text{ g Cm}^{-2} \text{ yr}^{-1}$  (Fig. 2b); and the  $NPP_p$  was in a declining trend in most of the QTP except for the middle or the southern margin (Fig. 3d). Furthermore,  $NPP_h$  also decreased at a rate of  $-1.85 \text{ g Cm}^{-2} \text{ yr}^{-1}$  (Fig. 2c), and the decreasing  $NPP$  area distributed in the middle west and north of the QTP, but the east and west margins exhibited an increasing trend (Fig. 3f). Overall, the decreasing rate of  $NPP_h$  change was greater than that of  $NPP_p$  change, this led to an increasing in  $NPP_A$  change trend in the latter ten years. In this period of 2001 to 2011, the Chinese government has enforced a national conservation policy on payment for supporting the ecological project Grazing Withdrawal Program (GWP) over the north China grassland around 2003, which brought about the evidently declining the number of livestock and implementation of many large scale ecological projects, such as fencing degrading grassland, ecological compensation and restoring the land cover vegetation (Feng et al., 2013; Mu et al., 2013). All the policies and projects enforcements help reducing the grazing pressure over the QTP, leading to the  $NPP_A$  increasing under the circumstances of both the  $NPP_p$  and  $NPP_h$  decreasing caused by climate warm-dry and human activities disturbances respectively.

### 3.4. The causes of $NPP_A$ change in two periods

As the annual  $NPP_A$  has been driven by two different drivers in 1981–2001 and 2001–2011 separately, the area percentage of  $NPP_A$  change caused by different reasons would also has been changed in the two periods. Comparing the absolute value of the slopes of  $NPP_p$  and  $NPP_h$  in every pixel by using the mathematical regulation in the table over the QTP in the last thirty years (Table 1), we can find where and how large of the determinants for  $NPP_A$  change in the past. From 1982 to 2001, most of the alpine grassland  $NPP_A$  increment area was caused by climate change; only a small area was in a decreasing trend or remaining unchanged in the middle-east and north margin of the QTP (Fig. 4 a). Meanwhile, in the south-east and north margin of the QTP, human activities caused regional  $NPP_A$  to decline, but it led to a regional  $NPP_A$  increase in the middle-east (Fig. 4a). From 2001 to 2011, most of the grassland  $NPP_A$  in the QTP was increasing, which mostly occurred to the east of the QTP. In the middle of the eastern QTP, the grassland  $NPP_A$  increased because of climate change, but the  $NPP_A$  increased as a result of a  $NPP_h$  decrease in the south and north-east. However, the grassland  $NPP$  mostly decreased in the west of the QTP, much of which was

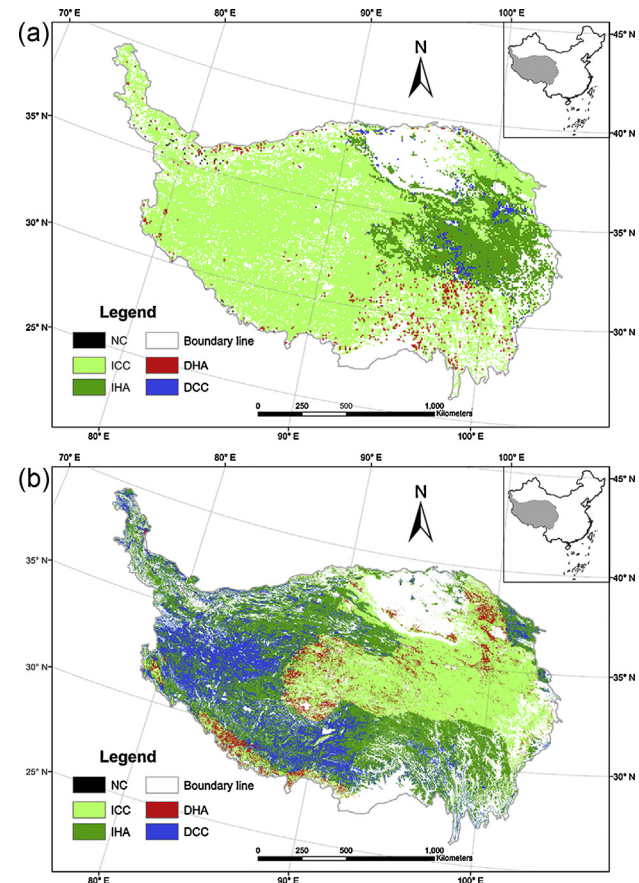


**Fig. 4.** Spatial distribution of different causes for alpine grassland NPP change in the periods 1982–2001 (a) and 2001–2011 (b). Note: NC is  $NPP_A$  had no change; ICC is  $NPP_A$  increased due to climate change; IHA is  $NPP_A$  increased due to human activities; DCC is  $NPP_A$  decreased due to climate change and DHA is  $NPP_A$  decreased due to human activities.

caused by climate change and some of which was caused by human activities, which occurred in the south, middle and north-east of the QTP and fitted with the population distribution (Fig. 4b). The  $NPP_h$  has increased more in the last ten years than in the previous twenty years, and increases more from east to west.

Calculating the area percentages of the factors that led to the alpine grassland  $NPP_A$  change in the two periods, we can compare and analyze the area percentages for climate change and human activities and summarize the developing tendency pattern of the two determinants of alpine grassland  $NPP_A$ , then providing a scientific basis for regional alpine grassland ecosystem management over the QTP. The statistical data showed the following: there was little change in the  $NPP_A$  no-change area between the two periods 1982–2001 and 2001–2011, increasing from 0.22% to 0.33%; the  $NPP_A$  increase due to climate change (ICC) percentage largely decreased from 78.03% to 32.87%; the  $NPP_A$  increase due to human activities (IHA) increased from 17.67% to 37.90%; the  $NPP_A$  decrease due to climate change (DCC) increased from 1.59% to 23.82%; and the  $NPP_A$  decrease due to climate change (DHA) increased from 2.49% to 5.08% (Table 2). Overall, the total area percentage of  $NPP_A$  change caused by climate change, including ICC and DCC, declined from 79.62% to 56.59%, but that percentage resulting from human activities, including IHA and DHA, enhanced from 20.16% to 42.98% between the periods of 1982–2001 and 2001–2011. The effect of human activities on the alpine grassland ecosystem over the QTP significantly intensified in the latter period compared with the previous 20 years, and the climate change effect has been relatively mitigated or offset.

**Table 2**

The NPP<sub>A</sub> change area percentage in the periods 1982–2001 and 2001–2011.

NPP <sub>A</sub> change area	1982–2001 (%)	2001–2011 (%)
NC	0.22	0.33
ICC	78.03	32.87
IHA	17.67	37.90
DCC	1.59	23.82
DHA	2.49	5.08

## 4. Discussion

### 4.1. NPP<sub>P</sub> and climate change over the QTP

Simulated TEM NPP<sub>P</sub> prediction is only influenced by climatic factors and has been regarded as the maximum NPP of an ecosystem (Raich et al., 1991), which can be considered as the alpine grassland NPP<sub>P</sub> that is not disturbed by animals or anthropogenic activities over the QTP. However, most of the alpine grassland is distributed in semi-dry and dry areas over the QTP, and these areas are sensitive to precipitation and vulnerable to climate warming (Qin et al., 2013). In this study, the main driving force of the alpine grassland NPP<sub>P</sub> is annual precipitation, which is also the reason for NPP<sub>P</sub> decline as the rainfall decrease since 2000 (Fig. 5 a). The NPP<sub>P</sub> has a strong relationship with annual rainfall, but the rapidly

increasing temperature exerts complicated effects on the NPP<sub>P</sub> (Piao et al., 2012; Zhuang et al., 2010). In the latest 30 years, the interpolated meteorological dataset showed a more significant warming trend of about 0.06 °C per year ( $P < 0.001$ ) (Zhang et al., 2013b), which is approximately double the warming rate in the last 50 years over the QTP. However, the rainfall increasing trend in the same period was just only about 0.14 mm per year, which is about one-sixth of the rainfall rate in the last 50 years (Piao et al., 2012). Both the increasing warming trend and decreasing rainfall trend may suggest that the warming and drying phenomena over the QTP were more serious in the past 30 years than that of latest 50 years, which could make the alpine grassland ecosystem more vulnerable to climate warming and more sensitive to grassland degradation as a result of human activities.

### 4.2. Grazing pressure and climate change

The major anthropogenic activities over the QTP that can influence alpine grassland NPP are grazing and human-induced land cover change (Chen et al., 2013; Harris, 2010); the former is the dominant one and can lead to grassland degradation, even desertification in the plateau. However, it is not clear whether the number of livestock directly affects NPP<sub>H</sub> or whether there are other influencing factors, so we recorded the number of total livestock over the

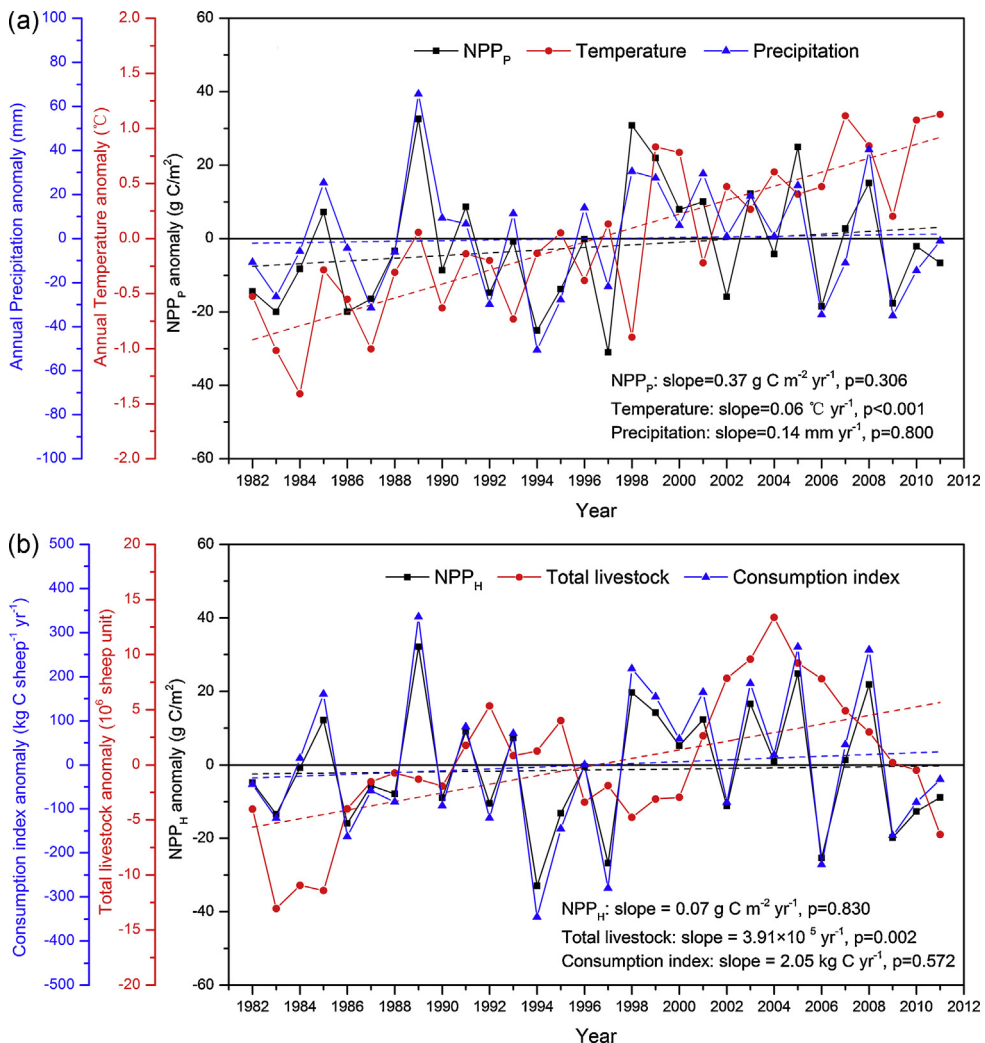


**Fig. 5.** Time series of (a) alpine grassland NPP<sub>P</sub>, annual temperature, and precipitation and (b) the NPP<sub>H</sub> consumption index per sheep unit, NPP<sub>H</sub>, and total livestock number anomalies over the QTP from 1982 to 2011. Note: the total number of livestock is the sum of horses, yaks, donkeys, and sheep. In calculating the NPP<sub>H</sub> consumption index per sheep unit, large animals, such as horses, were changed to standardized sheep units (e.g., one yak = four sheep).

QTP, which all the statistical data were obtained from the National Bureau of Statistics of China, and large animals such as cattle and horses are regarded as equivalent to four sheep units (Fan et al., 2010). We then estimated the average NPP consumption for one sheep unit over alpine grassland, calculated as the  $NPP_H$  amount consumed by per sheep unit in the 30-year period, and determined that consumption index was not a constant value but has slightly increased in the past 30 years, with the increasing rate of  $2.05 \text{ kg Cyr}^{-1}$  per sheep unit, and a total increase of about 15.67% (Fig. 5b). Moreover, the predicted  $NPP_H$  also enhanced in this thirty years, suggesting that grazing pressure over the alpine grassland ecosystem was a little increasing from 1982 to 2011 in generally. As the GWP implemented around 2003, the number of livestock come up to dramatically decrease since 2004, which also brought about a relatively decrease of  $NPP_H$  and its consumption index per sheep unit (Fig. 5b), letting alpine grassland ecosystem over the QTP with a slight recover from heavy grazing pressure.

As the  $NPP_H$  was relatively unrelated to the number of livestock over the QTP, but changed along with  $NPP_H$  consumption per sheep unit in the last 30 years (Fig. 5b), accompanying with the  $NPP_H$  has related with  $NPP_P$  (Fig. 2b and c), that could be deduced by alpine grassland  $NPP_H$  consumption per sheep unit also has a strong connection with the amount of rainfall in this arid and semi-arid plateau. The phenomenon could roughly be accounted for by the theory that animal consumption per sheep unit of grass biomass varies in different years, and the animals could eat more above-ground grass biomass in a good harvest year and less in a poor year, so to some extent natural laws maintain the grassland in such a condition whereby sufficient grass grows for the animals. However, with the dramatic growth in animal rearing, the grassland cannot meet the vast demand, so widespread degradation has occurred over the QTP. Furthermore, human-induced land cover change could induce retrogressive succession, whereby more inedible sedge grass species make up most of the alpine grassland, so there is a need for human intervention to eliminate the invading grass species or to reseed the local fine gramineous species to balance the natural ecosystem (Shang et al., 2012; Wang et al., 2013).

#### 4.3. Ecological projects achievements

The total number of livestock is the key to alpine grassland effective management over the QTP, which showed a significant increase in the last thirty years ( $P < 0.01$ , Fig. 5b). Though rearing livestock is the main source of income to local herdsman, increasing the number of animals also creates a potential threat to the alpine grassland ecosystem balance. So, in view of climate warming, it is both necessary and highly critical to evaluate alpine grassland ecosystem natural capacity and control the number of animals reared. The national policy of GWP and ecological compensation over the QTP, implemented around 2003, aimed for protecting degrading rangeland and controlling the number of animals bred within a proper level, then has led to an obvious decline in the  $NPP_H$  trend since 2004 (Fig. 5b). In this study, we can see that the IHA area increased obviously to 37.90% in the past 10 years, from 17.67% in the previous 20 years. Such positive effects of this grassland protection policy have also been found in Inner Mongolia and Loess plateau (Feng et al., 2013; Li et al., 2012; Mu et al., 2013). These studies findings indicate that the national ecological protection policy has achieved positive ecological effects in northern China and the QTP.

#### 5. Conclusions

In this study, we discriminated and quantified the effects of climate change and anthropogenic activities on alpine grassland ecosystem over the QTP, finding the different driving forces for the

actual  $NPP_A$  consistently enhanced in the periods of 1982–2001 and 2001–2011. Under the influences of climate change and human activities, the prime determinants of the increase in  $NPP_A$  in the two periods were changed. A warm-wet climate and less human activities caused a rapid increase in  $NPP_P$  and a relatively slow increase in  $NPP_H$ , which led to an  $NPP_A$  increase from 1982 to 2001. However, as the warm-dry climate decreased the alpine grassland  $NPP_P$  over the QTP from 2001 to 2011, marked human intervention on the alpine grassland ecosystem (fencing degrading grassland and reducing livestock number) played a much more important role in the grassland restoration, which still resulted in  $NPP_A$  increasing in this period. This implies that the obvious decline in the number of livestock animals and large-scale building the fences over the QTP alpine grassland in recent years relieved the grazing pressure of the rangeland, and indirectly caused an  $NPP_A$  increase in this latter 10 years period. Furthermore, for further fully and precisely separating the effects of climate change and human activities on ecosystem in sub-region, more field data and accurate process-based ecosystem models are needed.

#### Acknowledgements

This study was jointly supported by Chinese Academy of Sciences project (XDB03030400), the National Basic Research Program of China (No. 2010CB951704), and the National Sciences Foundation of China (41171044). The constructive comments and suggestions from anonymous reviewers are also highly appreciated.

#### References

- Aldous, A., Fitzsimons, J., Richter, B., Bach, L., 2011. Droughts, floods and freshwater ecosystems: evaluating climate change impacts and developing adaptation strategies. *Mar. Freshwater Res.* 62 (3), 223–231.
- Bai, Z.G., Dent, D.L., Olsson, L., Schaepman, M.E., 2008. Proxy global assessment of land degradation. *Soil Use Manage.* 24 (3), 223–234.
- Bartholomé, E., Belward, A.S., 2005. GLC2000: a new approach to global land cover mapping from Earth observation data. *Int. J. Remote Sens.* 26 (9), 1959–1977.
- Chen, H., et al., 2013. The impacts of climate change and human activities on biogeochemical cycles on the Qinghai–Tibetan plateau. *Global Change Biol.* 19 (10), 2940–2955.
- Consortium, P.K., 2013. Continental-scale temperature variability during the past two millennia. *Nat. Geosci.* 6, 339–347.
- DeFries, R., 2002. Past and future sensitivity of primary production to human modification of the landscape. *Geophys. Res. Lett.* 29 (7), 36–1–36–4.
- DeFries, R.S., Field, C.B., Fung, I., Collatz, G.J., Bounoua, L., 1999. Combining satellite data and biogeochemical models to estimate global effects of human-induced land cover change on carbon emissions and primary productivity. *Global Biogeochem. Cycles* 13 (3), 803–815.
- Du, M., Kawashima, S., Yonemura, S., Zhang, X., Chen, S., 2004. Mutual influence between human activities and climate change in the Tibetan plateau during recent years. *Global Planet Change* 41 (3–4), 241–249.
- Erb, K.-H., et al., 2009. Analyzing the global human appropriation of net primary production – processes, trajectories, implications: an introduction. *Ecol. Econ.* 69 (2), 250–259.
- Esser, G., 1987. Sensitivity of global carbon pools and fluxes to human and potential climatic impacts. *Tellus* 39B (3), 245–260.
- Fan, J.W., et al., 2010. Assessment of effects of climate change and grazing activity on grassland yield in the three rivers headwaters region of Qinghai–Tibet plateau, China. *Environ. Monit. Assess.* 170 (1–4), 571–584.
- Feng, X., Fu, B., Lu, N., Zeng, Y., Wu, B., 2013. How ecological restoration alters ecosystem services: an analysis of carbon sequestration in China's Loess plateau. *Sci. Rep.* 3, 2846.
- Field, C.B., 2001. Global change. Sharing the garden. *Science* 294 (5551), 2490–2491.
- Field, C.B., Randerson, J.T., Malmstrom, C.M., 1995. Global net primary production combining ecology and remote sensing. *Remote Sens. Environ.* 51 (1), 74–88.
- Gao, Q., et al., 2013. Effects of topography and human activity on the net primary productivity (NPP) of alpine grassland in northern Tibet from 1981 to 2004. *Int. J. Remote Sens.* 34 (6), 2057–2069.
- Gao, Y., et al., 2012. Vegetation net primary productivity and its response to climate change during 2001–2008 in the Tibetan plateau. *Sci. Total Environ.* 444, 356–362.
- Haberl, H., 1997. Human appropriation of net primary production as an environmental indicator: implications for sustainable development. *Roy. Swed. Acad. Sci.* 26 (3), 143–146.

- Haberl, H., et al., 2007. Quantifying and mapping the human appropriation of net primary production in earth's terrestrial ecosystems. *Proc. Natl. Acad. Sci. U.S.A.* 104 (31), 12942–12947.
- Harris, R.B., 2010. Rangeland degradation on the Qinghai–Tibetan plateau: a review of the evidence of its magnitude and causes. *J. Arid Environ.* 74 (1), 1–12.
- Jiang, Y., et al., 2012. Hyper-temporal remote sensing helps in relating epiphyllous liverworts and evergreen forests. *J. Veg. Sci.* 24 (2), 214–226.
- Jönsson, P., Eklundh, L., 2004. TIMESAT—a program for analyzing time-series of satellite sensor data. *Comput. Geosci.* 30 (8), 833–845.
- Krausmann, F., et al., 2013. Global human appropriation of net primary production doubled in the 20th century. *Proc. Natl. Acad. Sci. U.S.A.* 110 (25), 10324–10329.
- Lawler, J.J., 2009. Climate change adaptation strategies for resource management and conservation planning. *Ann. NY. Acad. Sci.* 1162, 79–98.
- Li, A., Wu, J., Huang, J., 2012. Distinguishing between human-induced and climate-driven vegetation changes: a critical application of RESTREND in inner Mongolia. *Landscape Ecol.* 27 (7), 969–982.
- Li, X., et al., 2011. Root biomass distribution in alpine ecosystems of the northern Tibetan plateau. *Environ. Earth Sci.* 64 (7), 1911–1919.
- Liu, Y., et al., 2012. Effects of plateau pika (*Ochotona curzoniae*) on net ecosystem carbon exchange of grassland in the three rivers headwaters region, Qinghai–Tibet, China. *Plant Soil* 366 (1–2), 1–14.
- Luck, G.W., 2007. The relationships between net primary productivity, human population density and species conservation. *J. Biogeogr.* 34 (2), 201–212.
- Ma, M., Wang, J., Wang, X., 2006. Advance in the inter-annual variability of vegetation and its relation to climate based on remote sensing. *J. Remote Sens.* 10 (3), 421–431 (in Chinese).
- Melillo, J.M., et al., 1993. Global climate change and terrestrial net primary production. *Nature* 363 (6424), 234–240.
- Mu, S., et al., 2013. Assessing the impact of restoration-induced land conversion and management alternatives on net primary productivity in inner Mongolian grassland, China. *Global Planet Change* 108, 29–41.
- Piao, S., et al., 2011. Altitude and temperature dependence of change in the spring vegetation green-up date from 1982 to 2006 in the Qinghai–Xizang plateau. *Agric. For. Meteorol.* 151 (12), 1599–1608.
- Piao, S., et al., 2012. Impacts of climate and CO<sub>2</sub> changes on the vegetation growth and carbon balance of Qinghai–Tibetan grasslands over the past five decades. *Global Planet Change* 98 (99), 73–80.
- Potter, C., 2004. Predicting climate change effects on vegetation, soil thermal dynamics, and carbon cycling in ecosystems of interior Alaska. *Ecol. Modell.* 175 (1), 1–24.
- Potter, C., et al., 2011. Carbon fluxes in ecosystems of yellowstone national park predicted from remote sensing data and simulation modeling. *Carbon Balance Manage.* 6 (3), 1–16.
- Potter, C.S., 1999. Terrestrial biomass and the effects of deforestation on the global carbon cycle. *Bioscience* 49 (10), 769–778.
- Potter, C.S., Klooster, S., Brooks, V., 1999. Interannual variability in terrestrial net primary production: exploration of trends and controls on regional to global scales. *Ecosystems* 2 (1), 36–48.
- Potter, C.S., et al., 1993. Terrestrial ecosystem production: a process model based on global satellite and surface data. *Global Biogeochem. Cycles* 7 (4), 811–841.
- Prince, S.D., Wessels, K.J., Tucker, C.J., Nicholson, S.E., 2007. Desertification in the Sahel: a reinterpretation of a reinterpretation. *Global Change Biol.* 13 (7), 1308–1313.
- Qin, Y., Yi, S., Ren, S., Li, N., Chen, J., 2013. Responses of typical grasslands in a semi-arid basin on the Qinghai–Tibetan plateau to climate change and disturbances. *Environ. Earth Sci.*, 1–11.
- Qiu, J., 2007. Riding on the roof of the world. *Nature* 449 (7161), 398–402.
- Qiu, J., 2008. The third pole. *Nature* 454 (7203), 393–396.
- Raich, J.W., et al., 1991. Potential net primary productivity in South America: application of a global model. *Ecol. Appl.* 1 (4), 399–429.
- Raupach, M.R., Quéré, C.L., Peters, G.P., Canadell, J.G., 2013. Anthropogenic CO<sub>2</sub> emissions. *Nat. Clim. Change* 3 (7), 603–604.
- Rojstaczer, S., Sterling, S.M., Moore, N.J., 2001. Human appropriation of photosynthesis products. *Science* 294 (5551), 2549–2552.
- Shang, Z.H., Yang, S.H., Shi, J.J., Wang, Y.L., Long, R.J., 2012. Seed rain and its relationship with above-ground vegetation of degraded Kobresia meadows. *J. Plant Res.* 126 (1), 63–72.
- Stow, D., et al., 2003. Variability of the seasonally integrated normalized difference vegetation index across the north slope of Alaska in the 1990. *Int. J. Remote Sens.* 24 (5), 1111–1117.
- Tian, H., et al., 1998. Effect of interannual climate variability on carbon storage in Amazonian ecosystems. *Nature* 396 (6712), 664–667.
- Vignola, R., Locatelli, B., Martinez, C., Imbach, P., 2009. Ecosystem-based adaptation to climate change: what role for policy-makers, society and scientists? *Mitig. Adapt. Strat. Glob.* 14 (8), 691–696.
- Vitousek, P.M., Ehrlich, P.R., Ehrlich, A.H., Matson, P.A., 1986. Human appropriation of the products of photosynthesis. *BioScience* 36 (6), 368–373.
- Wang, J., et al., 2013. Causes and restoration of degraded alpine grassland in northern Tibet. *J. Res. Ecol.* 4 (1), 43–49.
- Wessels, K.J., Prince, S.D., Frost, P.E., van Zyl, D., 2004. Assessing the effects of human-induced land degradation in the former homelands of northern South Africa with a 1 km AVHRR NDVI time-series. *Remote Sens. Environ.* 91 (1), 47–67.
- Wessels, K.J., et al., 2007. Can human-induced land degradation be distinguished from the effects of rainfall variability? A case study in South Africa. *J. Arid Environ.* 68 (2), 271–297.
- Wessels, K.J., Prince, S.D., Reshef, I., 2008. Mapping land degradation by comparison of vegetation production to spatially derived estimates of potential production. *J. Arid Environ.* 72 (10), 1940–1949.
- Wu, J., et al., 2013. Grazing-exclusion effects on aboveground biomass and water-use efficiency of alpine grasslands on the Northern Tibetan plateau. *Rangeland Ecol. Manag.* 66 (4), 454–461.
- Wu, Y., et al., 2009. Partitioning pattern of carbon flux in a Kobresia grassland on the Qinghai–Tibetan plateau revealed by field 13C pulse-labeling. *Global Change Biol.* 16 (8), 2322–2333.
- Xu, D., Kang, X., Liu, Z., Zhuang, D., Pan, J., 2009. Assessing the relative role of climate change and human activities in sandy desertification of Ordos region, China. *Sci. China Ser. D: Earth Sci.* 52 (6), 855–868 (in Chinese).
- Yang, K., et al., 2011. Response of hydrological cycle to recent climate changes in the Tibetan plateau. *Clim. Change* 109 (4), 517–534.
- Yao, T., et al., 2012. Third pole environment (TPE). *Environ. Dev.* 3, 52–64.
- Yu, C., et al., 2012. Ecological and environmental issues faced by a developing Tibet. *Environ. Sci. Technol.* 46 (4), 1979–1980.
- Zhang, G., Zhang, Y., Dong, J., Xiao, X., 2013a. Green-up dates in the Tibetan plateau have continuously advanced from 1982 to 2011. *Proc. Natl. Acad. Sci. U.S.A.* 110 (11), 4309–4314.
- Zhang, X., Zhang, Y., Zhou, Y., 2000. Measuring and modelling photosynthetically active radiation in Tibet plateau during April–October. *Agric. For. Meteorol.* 102 (2–3), 207–212.
- Zhang, Y., et al., 2013b. Spatial and temporal variability in net primary production (NPP) of alpine grassland on Tibetan Plateau from 1982 to 2009. *Acta Geogr. Sin.* 68 (9), 1197–1211 (in Chinese).
- Zhou, C., Ouyang, H., Wang, X., Watanabe, M., Sun, Q., 2004. Estimation of net primary productivity in Tibetan plateau. *Acta Geogr. Sin.* 59 (1), 74–79 (in Chinese).
- Zhuang, Q., et al., 2010. Carbon dynamics of terrestrial ecosystems on the Tibetan plateau during the 20th century: an analysis with a process-based biogeochemical model. *Global Ecol. Biogeogr.* 19 (5), 649–662.